International Conference on Mathematics, Computational Methods & Reactor Physics (M&C 2009)
Saratoga Springs, New York, May 3-7, 2009, on CD-ROM, American Nuclear Society, LaGrange Park, IL (2009)

A TIME-DEPENDENT METHOD OF CHARACTERISTICS FOR 3D NUCLEAR REACTOR KINETICS APPLICATIONS

J. Bryce Taylor
P.O. Box 164, Milesburg, PA 16853
bryce@milesburg-scientific.com

Anthony J. Baratta
Professor Emeritus of Nuclear Engineering
The Pennsylvania State University
ab2@psu.edu

ABSTRACT

The authors have previously proposed application of the method of characteristics to a 3D nuclear reactor kinetics methodology and have demonstrated the potential feasibility and efficiency of ray tracing and steady state analysis for 3D geometries. One possible approach to the derivation of a time-dependent characteristics formulation, which applies fully implicit time-differencing to the method of characteristics, is now presented. The fully implicit method of characteristics has been successfully implemented into the MOCK-3D reactor kinetics code package, without computational acceleration or thermal-hydraulic feedback; however, a unique numerical stability is discussed that could necessitate the investigation of alternative temporal discretization techniques. Assessment of MOCK-3D is pursued via application to the 2D TWIGL seed/blanket problem. Because the computation expense of a MOCK-3D calculation is exorbitant at this early stage in development, spatial resolution and the accuracy of results are severely limited; nonetheless, the fully implicit time-dependent method of characteristics is shown to capture the dominant physical phenomena of the 2D TWIGL problem. This analysis provides the first evidence of feasibility for a time-dependent method of characteristics calculation, although practical application will require the introduction of substantial additional sophistication via computational acceleration and/or parallel processing.

Key Words: method of characteristics, time-dependent neutron transport, 3D nuclear reactor kinetics

1. INTRODUCTION

A nuclear reactor kinetics code that can evaluate time-dependent changes to the neutron flux is an essential component in the suite of tools available for nuclear reactor analysis. Commercial reactor kinetics codes have traditionally relied on nodal diffusion theory to perform such computations; however, the accuracy of a diffusion theory solution is limited for a variety of circumstances: when strong material and/or flux gradients are present, when neutron streaming is significant, or when neutron scattering contains a strongly anisotropic component. As such situations have become increasingly more common in commercial nuclear reactor analysis, recent investigations have pursued an advanced reactor kinetics methodology that utilizes more accurate neutron transport methods. Time-dependent formulations for finite-differenced discrete ordinates (S_N) methods [1,2], spherical harmonics (P_n) methods [3], simplified spherical harmonics (SP_N) methods [4,5], and variational methods [6] have all been investigated. The authors have proposed the addition of the method of characteristics to this list of transport methods that could be utilized in advanced nuclear reactor kinetics analysis [7].

The method of characteristics is preferred to other transport methods for use in lattice physics codes due to its superior accuracy in problems with extremely detailed and heterogeneous material configurations. The method of characteristics could be similarly applicable to certain time-dependent phenomena – such as near the tip of a control rod during a rod ejection transient [8] – where spatial heterogeneity is a significant factor. Such an application would necessitate the modeling of three-dimensional (3D) geometries, however, and for reasons of computational expense the method of characteristics traditionally has been limited to two-dimensional (2D) geometry. Recent advances have made feasible an explicit 3D method of characteristics-based lattice physics calculation [9-12] and in Reference 7 these experiences were applied to the development of a 3D ray tracing algorithm and steady state method of characteristics solver for use in a 3D nuclear reactor kinetics methodology. The next required component in such a methodology – the derivation and numerical computation of a time-dependent formulation for the method of characteristics – is presented here.

As no other investigation into a time-dependent method of characteristics has been presented in recent literature, the development of a complete and practically applicable reactor kinetics package based on the method of characteristics poses a significant undertaking and is beyond the scope of this work. Instead, the goals of the initial study are to demonstrate the potential feasibility of such an approach and to point to the most critical needs of future research. To meet this goal of "proof-in-principle", simple and well-understood methods are used where possible and more advanced techniques – including thermal-hydraulic coupling, advanced time-dependent methods to address stiffness, computational acceleration, and parallel processing – are not included. In Reference 7 several additional problem simplifications were introduced that minimize computational inefficiency at the cost of accuracy in the results. Similar choices are made in the theoretical derivations and practical implementation that are described below.

Section 2 presents a derivation of one possible formulation for a time-dependent method of characteristics, using the well-known backward differencing approximation that yields a fully implicit solution to the time-dependent characteristic equation. Section 3 describes iterative numerical methods that are used to solve this equation, as implemented in the MOCK-3D reactor kinetics package. A discussion of numerical stability of the fully implicit method of characteristics is also presented, as this formulation raises unique issues that have not been previously encountered for other transport methods. Finally, in Section 4, the fully implicit method of characteristics is applied to the 2D TWIGL seed/blanket problem to provide an initial developmental assessment. The derivations, results, and discussion presented in this paper are extracted from a more thorough study that has been recently published in Reference 13.

2. DERIVATION OF A FULLY IMPLICIT FORMULATION FOR THE TIME-DEPENDENT METHOD OF CHARACTERISTICS

Derivation of the fundamental equations for a time-dependent method of characteristics closely parallels development of the steady state formulation and will utilize many of the same techniques and approximations. For example, both formulations employ the same transformation from Cartesian to Lagrangian spatial coordinates, discretization of the spatial, angular, and energy domains, and introduce an appropriate approximation to describe the neutron

source term. As such methods are well understood and have been investigated at length elsewhere, these will not be discussed. Instead, emphasis is placed on differences between the steady state and time-dependent method of characteristics and on circumstances that are unique to the time-dependent formulation.

The steady state method of characteristics proceeds by discretizing a Lagrangian formulation of the neutron transport equation, yielding an ordinary differential equation,

$$\frac{d}{ds}\Phi_{m,n,p}^{i,g}(s)+\overline{\Sigma}_{tr}^{i,g}\Phi_{m,n,p}^{i,g}(s)=\frac{1}{4\pi}\cdot\left\{\sum_{g'=1}^{G}\overline{\Sigma}_{s}^{i,g'\to g}\overline{\phi}^{i,g'}+\frac{\chi^{g}}{k_{\infty}}\sum_{g'=1}^{G}\overline{\nu\Sigma}_{f}^{i,g'}\overline{\phi}^{i,g'}\right\}=\overline{Q}^{i,g}, \qquad (1)$$

which is solvable via direct integration over the one-dimensional spatial variable, s. If a time-dependent method of characteristics is sought this derivation must be modified by a) omitting the steady state eigenvalue, k_{eff}, and retaining the term from the general neutron transport equation that describes the time rate-of-change of the neutron angular flux, $\partial\Phi/\partial t$; b) separating the fission neutron source into prompt and delayed components; and c) introducing a second equation to describe the time-dependence of the delayed neutron precursor concentrations, C_l. The result is a set of partial differential equations,

$$\begin{aligned}&\frac{1}{\mathrm{v}^{g}}\frac{\partial}{\partial t}\Phi_{m,n,p}^{i,g}(s,t)+\frac{\partial}{\partial s}\Phi_{m,n,p}^{i,g}(s,t)+\overline{\Sigma}_{tr}^{i,g}\Phi_{m,n,p}^{i,g}(s,t)\\&=\frac{1}{4\pi}\left\{\sum_{g'=1}^{G}\overline{\Sigma}_{s}^{i,g'\to g}\overline{\phi}^{i,g'}(t)+\chi_{p}^{g}(1-\beta)\sum_{g'=1}^{G}\overline{\nu\Sigma}_{f}^{i,g'}\overline{\phi}^{i,g'}(t)+\chi_{d}^{g}\sum_{l}\lambda_{l}\overline{C}_{l}^{i}(t)\right\}\end{aligned} \qquad (2)$$

and

$$\frac{\partial}{\partial t}\overline{C}_{l}^{i}(t)+\lambda_{l}\overline{C}_{l}^{i}(t)=\beta_{l}\sum_{g'=1}^{G}\overline{\nu\Sigma}_{f}^{i,g'}\overline{\phi}^{i,g'}(t), \qquad (3)$$

that represent a Lagrangian analogue to the multi-group reactor kinetics equations. The presence of bars over each of the scalar quantities in Equations (1), (2), and (3) indicates that the constant source approximation has been applied, while the spatial indices are defined for 3D geometry as defined in Reference 7. The notation used throughout this derivation is otherwise consistent with literature on the method of characteristics and time-dependent neutron transport.

Solution of Equations (2) and (3) requires the introduction of one of the direct or indirect methods that have been developed for use with nodal diffusion theory or other time-dependent transport methods [14], although not all of these methods are appropriate for use in the initial development of a time-dependent method of characteristics. To avoid unnecessary complexity in the resulting equations and to minimize computational expense, one of the simplest yet most well understood methods – the Θ-Method [15] – is selected for this initial investigation. Specifically, two particular Θ-Method formulations commonly employed for new methods development have been investigated: the explicit Euler, or forward-differencing, approximation and the implicit

Euler, or backward differencing, approximation. As discussed in Reference 13, an explicit solution to the time-dependent characteristic equation was found to be impractical due to well-known problems regarding numerical instability as well as unique incompatibilities with the method of characteristics. A fully implicit formulation is pursued below.

If the backward differencing approximation is applied to the time-dependent characteristic equation, Equation (2) becomes

$$\begin{aligned}&\frac{\Phi_{m,n,p}^{i,g}(s)\Big|^{T+1}-\Phi_{m,n,p}^{i,g}(s)\Big|^{T}}{\mathrm{v}^{g}\Delta t}+\frac{d}{ds}\Phi_{m,n,p}^{i,g}(s)\Big|^{T+1}+\overline{\Sigma}_{tr}^{i,g}\,\Phi_{m,n,p}^{i,g}(s)\Big|^{T+1}\\&=\sum_{g'=1}^{G}\overline{\Sigma}_{s}^{i,g'\to g}\,\overline{\phi}^{i,g'}\Big|^{T+1}+\chi_{p}^{g}(1-\beta)\sum_{g'=1}^{G}\overline{\nu\Sigma}_{f}^{i,g'}\,\overline{\phi}^{i,g'}\Big|^{T+1}+\chi_{d}^{g}\sum_{l}\lambda_{l}\,\overline{C}_{l}^{i}\Big|^{T+1}\end{aligned}. \tag{4}$$

Applying the analogous approximation to Equation (3) yields the backward-differenced precursor equation,

$$\frac{\overline{C}_{l}\Big|^{T+1}-\overline{C}_{l}\Big|^{T}}{\Delta t}+\lambda_{l}\,\overline{C}_{l}\Big|^{T+1}=\beta_{l}\sum_{g'=1}^{G}\overline{\nu\Sigma}_{f}^{g'}\,\overline{\phi}^{g'}\Big|^{T+1}. \tag{5}$$

Equation (5) can be rearranged to solve for $\overline{C}_{l}\Big|^{T+1}$ and substituted into Equation (4), yielding a single equation,

$$\frac{d}{ds}\Phi_{m,n,p}^{i,g}(s)\Big|^{T+1}+\tilde{\overline{\Sigma}}_{tr}^{i,g}\,\Phi_{m,n,p}^{i,g}(s)\Big|^{T+1}=\tilde{\overline{Q}}^{i,g}, \tag{6}$$

where the effective transport cross section is defined to be

$$\tilde{\overline{\Sigma}}_{tr}^{i,g}=\left(\frac{1}{\mathrm{v}^{g}\Delta t}+\overline{\Sigma}_{tr}^{i,g}\right) \tag{7}$$

and the total effective neutron source term is given by

$$\begin{aligned}\tilde{\overline{Q}}^{i,g}&=\overline{Q}^{i,g}+\frac{\Phi_{m,n,p}^{i,g}(s)\Big|^{T}}{\mathrm{v}^{g}\Delta t}=\overline{Q}_{scatter}^{i,g}+\overline{Q}_{prompt}^{i,g}+\overline{Q}_{delay}^{i,g}+\frac{\Phi_{m,n,p}^{i,g}(s)\Big|^{T}}{\mathrm{v}^{g}\Delta t}\\&=\frac{1}{4\pi}\left\{\begin{array}{l}\displaystyle\sum_{g'=1}^{G}\overline{\Sigma}_{s}^{i,g'\to g}\,\overline{\phi}^{i,g'}\Big|^{T+1}+\chi_{p}^{g}(1-\beta)\sum_{g'=1}^{G}\overline{\nu\Sigma}_{f}^{i,g'}\,\overline{\phi}^{i,g'}\Big|^{T+1}\\ \displaystyle+\chi_{d}^{g}\sum_{l}\lambda_{l}\left[\gamma_{l}\,\overline{C}_{l}\Big|^{T}+\gamma_{l}\beta_{l}\Delta t\sum_{g'=1}^{G}\overline{\nu\Sigma}_{f}^{g'}\,\overline{\phi}^{g'}\Big|^{T+1}\right]\end{array}\right\}+\frac{\Phi_{m,n,p}^{i,g}(s)\Big|^{T}}{\mathrm{v}^{g}\Delta t},\end{aligned} \tag{8}$$

where $\gamma_l = (1+\lambda_l \Delta t)^{-1}$. Equation (6) is identical in form to the steady state characteristic equation, Equation (1), and can be solved using the same spatial integration technique. The general solution to Equation (6) will be

$$\begin{aligned}\Phi_{m,n,p}^{i,g}(s)\Big|^{T+1} &= \Phi_{m,n,p}^{i,g}\Big|_{in}^{T+1} e^{-\tilde{\Sigma}_{tr}^{i,g}[s-s_{in}]} \\ &+ \int_{s_{in}}^{s}\left[\overline{Q}^{i,g} + \frac{1}{\mathrm{v}^g \Delta t}\Phi_{m,n,p}^{i,g}(s')\Big|^{T}\right] e^{-\tilde{\Sigma}_{tr}^{i,g}[s'-s_{in}]} ds' .\end{aligned} \tag{9}$$

Resolution of the source-term integral on the right-hand side of Equation (9) is complicated by the presence of the term $\Phi_{m,n,p}^{i,g}(s)\Big|^{T}$, as the continuous spatial dependence of the neutron angular flux during the previous time step is unknown. A similar problem is encountered by the steady state method of characteristics, as continuous spatial dependence of the total neutron source term, $Q^{i,g}(s)$, complicates integration of the steady state characteristic equation. This issue is traditionally resolved via the introduction of an approximation to account for this spatial dependence – either by treating the total neutron source as constant in each cell (step characteristics) or as a linear function of position within the cell and/or along cell boundaries (linear characteristics). A similar set of approximations can be introduced to simplify spatial dependence of the neutron angular flux in Equation (9). The simplest approximation is to assume that the neutron angular flux is constant along a particular track,

$$\Phi_{m,n,p}^{i,g}(s')\Big|^{T} \Rightarrow \overline{\Phi}_{m,n,p}^{i,g}\Big|^{T}, \tag{10}$$

where $\overline{\Phi}_{m,n,p}^{i,g}$ is equivalent to the track-averaged angular flux and can be calculated as in the steady state method of characteristics according to

$$\overline{\Phi}_{m,n,p}^{i,g}\Big|^{T} = \frac{\overline{Q}^{i,g}}{\overline{\Sigma}_{tr}^{i,g}} + \frac{\Phi_{m,n,p}^{i,g}\Big|_{in}^{T} - \Phi_{m,n,p}^{i,g}\Big|_{out}^{T}}{\overline{\Sigma}_{tr}^{i,g}\Delta s_{m,n,p}} . \tag{11}$$

With this substitution, the integral in Equation (9) can now be resolved, yielding

$$\begin{aligned}\Phi_{m,n,p}^{i,g}\Big|_{out}^{T+1} &= \Phi_{m,n,p}^{i,g}\Big|_{in}^{T+1} e^{-\tilde{\Sigma}_{tr}^{i,g}\Delta s_{m,n,p}} \\ &+ \frac{1}{\tilde{\Sigma}_{tr}^{i,g}}\left[\overline{Q}^{i,g} + \left(\frac{1}{\mathrm{v}^g \Delta t}\right)\overline{\Phi}_{m,n,p}^{i,g}\Big|^{T}\right]\left(1 - e^{-\tilde{\Sigma}_{tr}^{i,g}\Delta s_{m,n,p}}\right).\end{aligned} \tag{12}$$

The assumption that neutron angular flux will be constant along a track segment is over-restrictive and would yield a trivial solution if extended to the full transport problem; i.e. an unvarying angular flux distribution across the entire problem space. An improved approximation

that allows for spatial variation is to assume that $\Phi^{i,g}_{m,n,p}(s)$ is a linear function of position along the track,

$$\Phi^{i,g}_{m,n,p}(s)\Big|^{T} = \Phi^{i,g}_{m,n,p}\Big|^{T}_{in} + \left[\frac{\Phi^{i,g}_{m,n,p}\Big|^{T}_{out} - \Phi^{i,g}_{m,n,p}\Big|^{T}_{in}}{\Delta s_{m,n,p}}\right]\left[s - s_{in}\right]. \tag{13}$$

Upon inserting Equation (13) into Equation (9), the neutron angular flux at the location where a track segment exits the 3D cell is found to be

$$\begin{aligned}\Phi^{i,g}_{m,n,p}\Big|^{T+1}_{out} &= e^{-\tilde{\Sigma}^{i,g}_{tr}\Delta s_{m,n,p}}\,\Phi^{i,g}_{m,n,p}\Big|^{T+1}_{in} + \left(\frac{1}{\tilde{\Sigma}^{i,g}_{tr}}\right)\left(1-e^{-\tilde{\Sigma}^{i,g}_{tr}\Delta s_{m,n,p}}\right)\overline{Q}^{i,g} \\ &+\left(\frac{1}{\mathrm{v}^{g}\Delta t}\right)\left(\frac{1}{\tilde{\Sigma}^{i,g}_{tr}}\right)\left\{1-\left(\frac{1}{\tilde{\Sigma}^{i,g}_{tr}\,\Delta s_{m,n,p}}\right)\left(1-e^{-\tilde{\Sigma}^{i,g}_{tr}\Delta s_{m,n,p}}\right)\right\}\Phi^{i,g}_{m,n,p}\Big|^{T}_{in} \\ &-\left(\frac{1}{\mathrm{v}^{g}\Delta t}\right)\left(\frac{1}{\tilde{\Sigma}^{i,g}_{tr}}\right)\left\{e^{-\tilde{\Sigma}^{i,g}_{tr}\Delta s_{m,n,p}}-\left(\frac{1}{\tilde{\Sigma}^{i,g}_{tr}\,\Delta s_{m,n,p}}\right)\left(1-e^{-\tilde{\Sigma}^{i,g}_{tr}\Delta s_{m,n,p}}\right)\right\}\Phi^{i,g}_{m,n,p}\Big|^{T}_{out}\end{aligned} \quad . \tag{14}$$

The two simple approximations described above were selected for initial investigation to minimize complexity of the resulting equations. Prior to implementation and assessment, however, it is unclear whether either of these approximations is appropriate for use in solving the time-dependent characteristic equation. In fact, as will be shown in Section 4, this issue cannot yet be fully resolved. If sensitivity to the order of the neutron angular flux approximation is found to be significant, a higher-order approximation may be required, such as an n^{th} order polynomial or exponential function. A more precise estimate of this term could also be derived via a Taylor polynomial expansion or recursive techniques.

3. NUMERICAL COMPUTATION OF THE FULLY IMPLICIT METHOD OF CHARACTERISTICS

Having derived a suitable set of equations to represent the time-dependent method of characteristics, a strategy for numerical solution must next be developed. To this end the fully implicit method of characteristics presented in Section 2 has been implemented into the 3D nuclear reactor kinetics code package MOCK-3D that was introduced in Reference 7. Most of the techniques used in the time-dependent characteristics solver, MOCK-3DK, have been developed and implemented previously for other fully implicit solutions to the neutron transport equation and these will be only briefly reviewed in Section 3.1. A more complete description of the MOCK-3D code package is presented in Reference 13. In Section 3.2 the problem of numerical stability is addressed in greater detail, as a unique problem is encountered that appears to be a direct consequence of applying the Θ-Method to a Lagrangian transport solution.

3.1 Numerical Computation of the Fully Implicit Method of Characteristics

A variety of iterative methods for numerical computation of an implicit solution to the neutron transport equation have been previously developed and applied to nodal diffusion theory or other advanced time-dependent transport methods. One of the most common and well understood of these techniques is fixed source iteration [16], which was selected for use in MOCK-3DK. In fixed source iteration the transport computation within each time step is recast into a pseudo-steady state eigenvalue problem; thus, many of the computational methods that have been previously developed for solution of the steady state transport equation can be applied with minimal modification. The most important steps in the fixed source iteration procedure, as implemented in MOCK-3DK, are briefly summarized below:

- To begin each time step the delayed neutron precursor concentrations are updated from the neutron source terms for the previous time step (or, in the first time step, are estimated from the initial equilibrium reactor state) and then held constant for the duration of that time step.

- Outer iteration begins by holding the total fission neutron source constant (prompt and delayed neutron components) and control passes to the inner iteration.

- Inner iteration is pursued for each energy group, beginning with the highest energy group, and upscattering is forbidden. The angular flux distribution for energy group g is calculated via the track-sweep technique illustrated in Figure 1. Angular flux calculations within the inner iterate use an appropriate solution for the backward-differenced characteristics equation – Equation (12) if the constant angular flux approximation is used or Equation (14) when using the linear angular flux approximation.

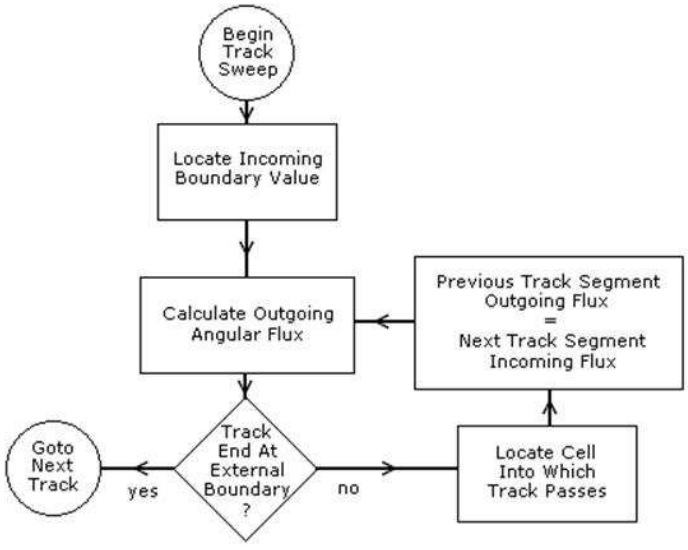

Figure 1: MOCK-3DK Track Sweep Procedure

- When the complete neutron angular flux distribution has been estimated for energy group g, the neutron scalar flux distribution and scattered neutron source term are updated and

convergence of the angular and scalar flux distributions is evaluated. When both distributions are fully converged, inner iteration is repeated for all lower energy groups.

- Upon completion of the inner iteration for all energy groups, outer iteration continues with a calculation of the total fission source for the j^{th} outer iterate in each cell, i, $F^{i(j)}$, which is used to update a fixed source eigenvalue, $\gamma^{(j)}$, according to

$$\gamma^{(j)} = \gamma^{(j-1)} \frac{\sum_i F^{i(j)}}{\sum_i F^{i(j-1)}} . \tag{15}$$

- It should be noted that in a steady state calculation the eigenvalue has a meaningful physical interpretation – i.e., the effective multiplication factor, k_{eff}. In a time-dependent calculation $\gamma^{(j)}$ has no comparable physical meaning and is used merely as a tool to evaluate convergence of the outer iterate. When the outer iterate is found to converge, the computation proceeds to the next time step.

The nested iteration procedures described above are repeated for each time step in sequence until the total problem time has elapsed. Because fixed iteration requires the equivalent of a full steady state computation for each time-step and any computation will include many such time steps, this initial implementation of the time-dependent method of characteristics is severely inefficient. While computational efficiency can be improved via the introduction of acceleration and/or parallel processing, such advanced computational techniques are not yet included and the modeling capability of MOCK-3DK is somewhat limited, as discussed in Section 4.

3.2 Numerical Stability of the Fully Implicit Method of Characteristics

It is well known that a fully implicit numerical solution to the time-dependent transport equation will be unconditionally stable for all but a few special circumstances (such as when extremely rapid temporal phenomena are observed); nonetheless, stiffness in the reactor kinetics equations necessitates a practical upper limit on time step size to avoid inaccuracies in the transport solution. When the backwards differencing approximation is applied to a method of characteristics transport solution, with its unique Lagrangian description of the spatial domain, a peculiar numerical instability is observed that also sets a lower limit on time step size. To illustrate this problem, the simplest formulation for the forward-differenced characteristic equation, Equation (12), is restated with most of the spatial, angular, and energy indices suppressed for clarity,

$$\begin{aligned}\Phi\big|_{out}^{T+1} &= \Phi\big|_{in}^{T+1} e^{-\left(\frac{1}{v\Delta t}+\bar{\Sigma}_{tr}\right)\Delta s} \\ &+ \left(\frac{\bar{Q}}{\bar{\Sigma}_{tr}}\right)\left(1-e^{-\left(\frac{1}{v\Delta t}+\bar{\Sigma}_{tr}\right)\Delta s}\right)+\left(\frac{1}{v^g\Delta t}\right)\left(\bar{\Phi}\Big|^{T}\right)\left(1-e^{-\left(\frac{1}{v\Delta t}+\bar{\Sigma}_{tr}\right)\Delta s}\right).\end{aligned} \tag{16}$$

Equation (16) represents the "constant angular flux" formulation, but the following observations will hold for the "linear angular flux" formulation as well. From previous experience with the steady state method of characteristics it is known that the probability that a neutron will not experience a collision during the time interval Δt as it traverses the track length Δs is given by $e^{-\left(\frac{1}{v\Delta t}+\bar{\Sigma}_{tr}\right)\Delta s}$ and, therefore, $1-e^{-\left(\frac{1}{v\Delta t}+\bar{\Sigma}_{tr}\right)\Delta s}$ is the probability that a neutron does experience a collision. Given these definitions, the three terms on the right hand side of Equation (16) can be interpreted physically as a neutron streaming term, a neutron source term, and a neutron loss term, respectively. As with the steady state characteristic equation, neutron balance is maintained where upscattering has been forbidden.

Of particular concern in Equation (16) is the occurrence of the term $1/v\Delta t$, which occurs twice: within each instance of the collision or non-collision probability and as a multiplier to the neutron loss term. In the latter case, where $1/v\Delta t$ appears within the loss term, a singularity occurs as $\Delta t \rightarrow 0$ where the loss term becomes infinite. If Δt is instead defined to be infinitesimally small but non-zero, the loss term will still be much larger than the source and streaming terms and will therefore dominate the solution to Equation (16). To avoid numerical instability due to this singularity, time step size must be defined to be larger than an undetermined minimum threshold value. This potential instability is of little practical importance, however, because in order for the singularity to adversely affect the results of an implicit calculation, Δt must be much smaller than would normally be desired. In fact, a similar singularity appears in spatial finite differencing forms of the reactor kinetics equations as well and has been successfully resolved in most instances.

The appearance of $1/v\Delta t$ within the collision and non-collision probability terms is more problematic and, because these terms are a direct result of the method of characteristics spatial integration technique, appears to be unique to a Lagrangian formulation for the time-dependent transport equation. In this case, if Δt is defined to be arbitrarily small then $1/v\Delta t$ will be much larger than $\bar{\Sigma}_{tr}$ and the relevant material effects – i.e., actual neutron collision events – are lost from the time-dependent transport solution, i.e.

$$\lim_{\Delta t \rightarrow 0} e^{-\left(\frac{1}{v\Delta t}+\bar{\Sigma}_{tr}\right)\Delta s} \Rightarrow e^{-\infty} \Rightarrow 0. \qquad (17)$$

A non-collision property of zero implies that every neutron undergoes collision, a result that would seem to be counter-intuitive. It could be logically deduced that as the time step size approaches zero then there will be insufficient time for neutron collision events to occur and, therefore, that the non-collision probability should approach a value of 1. This apparent inconsistency can be resolved by considering the physics of a time-dependent propagation problem. For an arbitrary but finite track length, Δs, a neutron with velocity, v, will require a an amount of time to traverse the entire length of this track that is given by

$$\widehat{\Delta t} = \frac{\Delta s}{v}. \qquad (18)$$

If $\Delta t < \widehat{\Delta t}$ then a neutron that originates at one endpoint of the track, Δs, will not have sufficient time reach the opposite endpoint of this track and will be lost, exactly as if it had undergone a collision event. In fact, as v^g represents the mean velocity for neutrons in energy group *g*, it is assumed that all neutrons in this group move at the same velocity and all neutrons are lost via this temporal pseudo-collision process.

The precise value for this minimum time step size, $\widehat{\Delta t}$ will depend on the material properties and spatial discretization of the particular problem of interest and will be bounded by the value of the longest track in the problem geometry and by the slowest (thermal) neutrons in the energy group structure. In an example where thermal neutron velocity is 10^5 cm/s and track length is 0.5 cm, $\widehat{\Delta t}$ is found to be on the order of 10^{-6} seconds. When combined with the typical upper time step limit of $\sim 10^{-3}$ seconds, the result is a relatively narrow window of possible time step sizes that may exclude the modeling of many rapid transients. Moreover, it should be noted that this numerical instability can be quite difficult to diagnose. In a typical method of characteristics problem specification, individual track lengths will vary up to an order of magnitude or more and may in some instances be larger than was specified by the user (a consequence of ray tracing procedures). If time step size is defined to be close to the lower limit, it is possible that instability could occur for only certain (the longest) track segments in the problem. As the numerical result of this instability is a null value for the angular flux at these locations, a thorough – and impractical – audit of the angular flux distribution may be required to ensure complete stability and accuracy of the method of characteristics solution. While the latter problem could be resolved via introduction of computational algorithms, the additional burdens placed on the user could complicate potential application of this methodology.

4. SOLUTION OF THE 2D TWIGL SEED/BLANKET PROBLEM VIA THE FULLY IMPLICIT METHOD OF CHARACTERISTICS

A survey of the literature reveals few time-dependent test problems that are suitable for the assessment of a time-dependent transport code such as MOCK-3DK. Many of the standard test problems or benchmark problems that are traditionally used to assess and validate reactor kinetics packages have been designed for the assessment of nodal diffusion theory and thus do not fully exercise the computational advantages of an advanced transport methodology. Additionally, most 3D reactor kinetics test problems include large spatial models and such features as reactivity feedback modeling. These whole-core problems are designed for the assessment of "best estimate" 3D reactor kinetics codes that will be applied to the analysis of commercial reactors and coupled to a simultaneous thermal-hydraulics calculation, but such problems are too large and complicated to be of use in the present work.

One problem that was found to be suitable for developmental assessment of MOCK-3DK is a 2D seed/blanket problem originally developed to validate the TWIGL diffusion theory code [17] that has since become a commonly used test problem for time-dependent diffusion theory and neutron transport codes. The TWIGL seed/blanket problem has not been standardized and a reference solution is not available; instead, code-to-code comparison is typically utilized to assess the accuracy of any particular solution. It will be shown, however, that the quality of a MOCK-3DK solution to the TWIGL problem is not sufficient to enable such an analysis.

Instead, the preliminary results presented and discussed below are used to make qualitative judgments about the feasibility of a time-dependent method of characteristics computation and to direct future research efforts.

4.1 2D TWIGL Seed/Blanket Problem Specifications

The 2D TWIGL problem models a 160.0 cm square reactor consisting of three material regions: unperturbed seed regions that contain the primary fissile material, an identically composed perturbed seed region to which time-dependent properties will be introduced, and a blanket region that contains fissile material and surrounds the core on all sides. The 2D model is laid out in quarter-core symmetry as shown in figure 2.

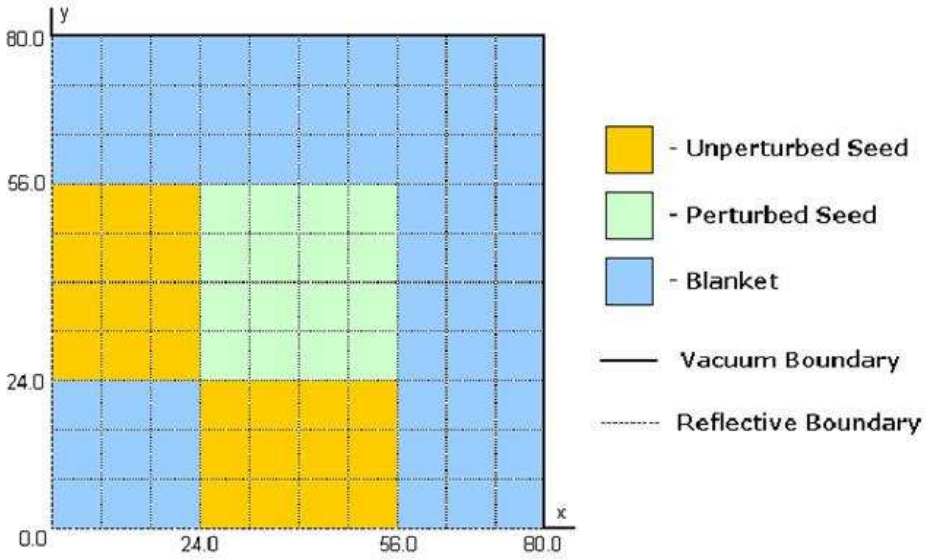

Figure 2: Problem Schematic for 2D TWIGL Seed/Blanket Problem

In its initial state, the hypothetical TWIGL reactor is slightly sub-critical (k_{eff} = 0.914193) and perturbed and unperturbed seed regions have identical material properties. The initial two energy group properties, one delay group constants, and additional kinetics parameters that have been adapted from Reference 17 are provided in Table 1 through Table 4.

Table 1: Material Properties for 2D TWIGL Seed/Blanket Problem, Seed Regions

Energy Group	$\Sigma_{tr,g}$ (cm^{-1})	$\Sigma_{a,g}$ (cm^{-1})	$\nu\Sigma_{f,g}$ (cm^{-1})	$\Sigma_{s,1\rightarrow g}$ (cm^{-1})	$\Sigma_{s,2\rightarrow g}$ (cm^{-1})
1	2.3810E-01	1.0000E-02	7.0000E-03	2.1810E-01	0.0000E+00
2	8.3333E-01	1.5000E-01	2.0000E-01	1.0000E-02	6.8333E-01

Table 2: Material Properties for 2D TWIGL Seed/Blanket Problem, Blanket Region

Energy Group	$\Sigma_{tr,g}$ (cm^{-1})	$\Sigma_{a,g}$ (cm^{-1})	$\nu\Sigma_{f,g}$ (cm^{-1})	$\Sigma_{s,1\rightarrow g}$ (cm^{-1})	$\Sigma_{s,2\rightarrow g}$ (cm^{-1})
1	2.5641E-01	8.0000E-03	3.0000E-03	2.3841E-01	0.0000E+00
2	6.6667E-01	5.0000E-02	6.0000E-02	1.0000E-02	6.1667E-01

Table 3: Neutron Generation Parameters for 2D TWIGL Seed/Blanket Problem

Energy Group	v_g (m/sec)	χ_{prompt} (-)	χ_{delay} (-)
1	1.0000E+07	1.0000E+00	1.0000E+00
2	2.0000E+05	0.0000E+00	0.0000E+00

Table 4: Kinetics Parameters for 2D TWIGL Seed/Blanket Problem

Delay Group	β_l (-)	λ_l (sec^{-1})
1	7.5000E-03	8.0000E-02

To perform a time-dependent calculation, the initial sub-critical equilibrium reactor state is made critical by dividing all of the fission cross sections, $\nu\Sigma_{f,g}$, by the given reference value for k_{eff}. Subsequently a delayed super-critical transient is initiated in the seed/blanket reactor by decreasing the thermal macroscopic transport cross-section, Σ_{tr}^2, in the perturbed seed region from the initial value of 0.83333 cm^{-1} to a final value of 0.82983 cm^{-1}. Most analyses of the TWIGL problem perform two separate transient calculations. In the first case, the perturbation is introduced as a step change at $t = 0.0$ sec. In the second case, a ramp change is introduced over the time period 0.0 sec < t < 0.2 sec. In both cases, the suggested total transient time is 0.5 seconds. In this study a third set of calculations is included – a series of null transient calculations whereby the initial reactor state is modeled in time without introducing any perturbation to the material configuration.

4.2 Initial Steady State Calculations

A MOCK-3D steady state calculation for the TWIGL problem geometry must be performed to determine the initial neutron angular flux and delayed neutron precursor concentration distributions, which are used to initialize all subsequent time-dependent MOCK-3DK computations. While assessment of the MOCK-3D steady state method of characteristics solver has been performed elsewhere, a brief examination of these initial computations will assist with the interpretation of time-dependent results that follow.

It was demonstrated in Reference 7 that computational cell size is the dominant user-defined parameter affecting the accuracy of a method of characteristics solution. To further assess this issue and to determine appropriate model parameters for subsequent time-dependent computations, steady state calculations for the TWIGL problem were performed for a range of spatial refinement as defined in Table 5.

Table 5: Cell and Lattice Sizes used in MOCK-3D for 2D TWIGL Steady State Calculation

Model	Cell Size (cm)	Lattice	Track Separation (cm)
1	0.5	160 x 160 x 160	0.10
2	1.0	80 x 80 x 80	0.20
3	2.0	40 x 40 x 40	0.40
4	4.0	20 x 20 x 20	0.80
5	8.0	10 x 10 x 10	1.60

All of the models described in Table 5 utilized S_4 level symmetric quadrature. Converged values for the effective multiplication factor, k_{eff}, are plotted in terms of cell size in Figure 3, where the red line indicates the given reference value for k_{eff}.

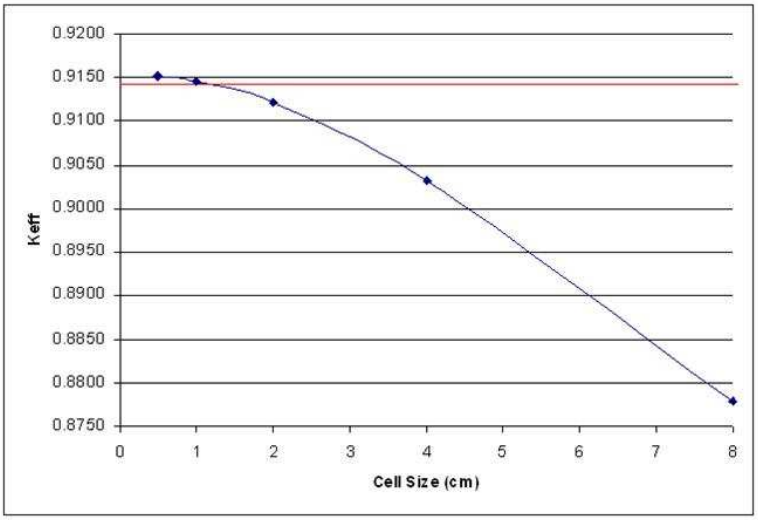

Figure 3: MOCK-3D k_{eff} versus Cell Size for 2D TWIGL Steady State Calculation

Figure 3 clearly demonstrates that for increasingly fine discretizations k_{eff} approaches the reference value asymptotically; however, accuracy degrades significantly for cell sizes larger than 1.0 cm. Such an observation suggests that spatial Model 1 (0.5 cm cell size) or Model 2 (1.0 cm cell size) would be most appropriate for use in the time-dependent calculations, although Model 3 (2.0 cm cell size) could be considered a reasonable compromise between the concerns of accuracy and computational efficiency. In practice, however, the computational expense of the MOCK-3DK time-dependent solver was extremely severe and only Model 5 (8.0 cm cell size) yielded a feasible time-dependent computation. To clarify the effects of this choice in spatial model, the two-group steady state neutron scalar flux distributions for Model 5 are compared to Model 2 in Figure 4 through Figure 7.

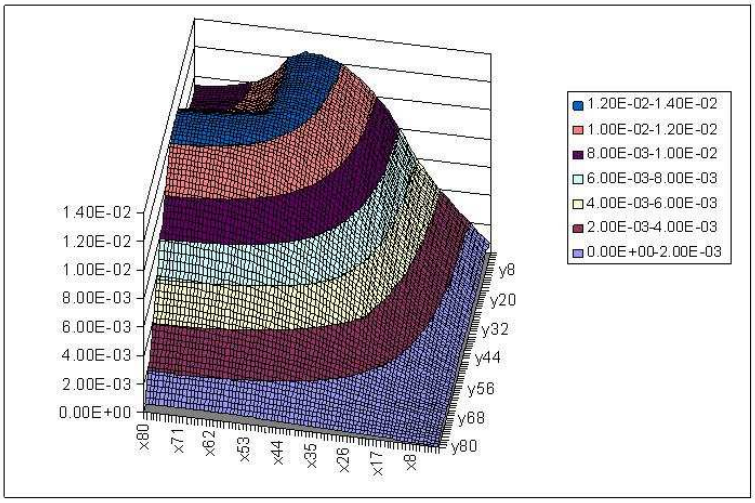

Figure 4: MOCK-3D Group 1 Steady State Scalar Flux Distribution for 2D TWIGL with 1.0 cm Cell Size

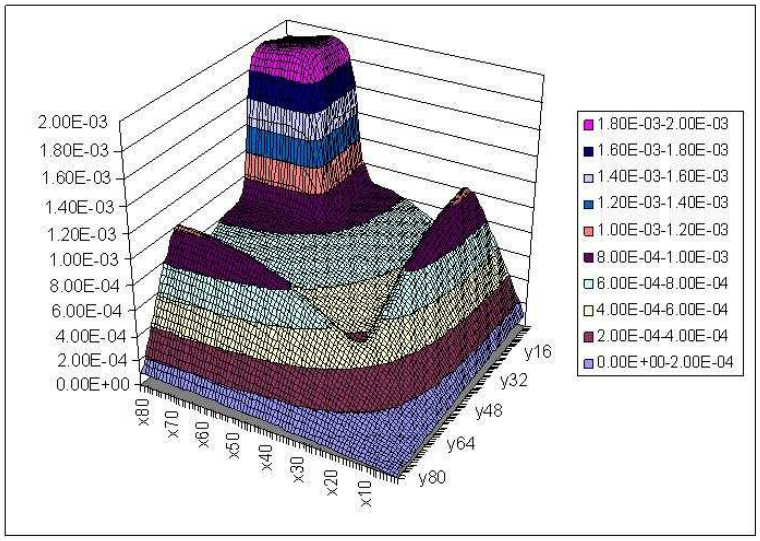

Figure 5: MOCK-3D Group 2 Steady State Scalar Flux Distribution for 2D TWIGL with 1.0 cm Cell Size

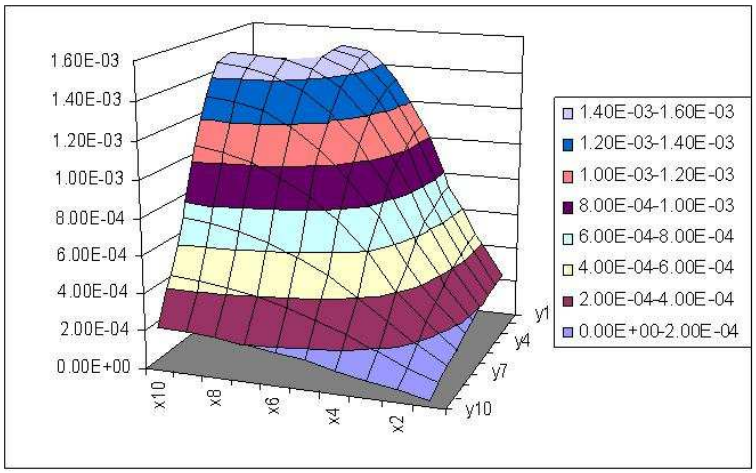

Figure 6: MOCK-3D Group 1 Steady State Scalar Flux Distribution for 2D TWIGL with 8.0 cm Cell Size

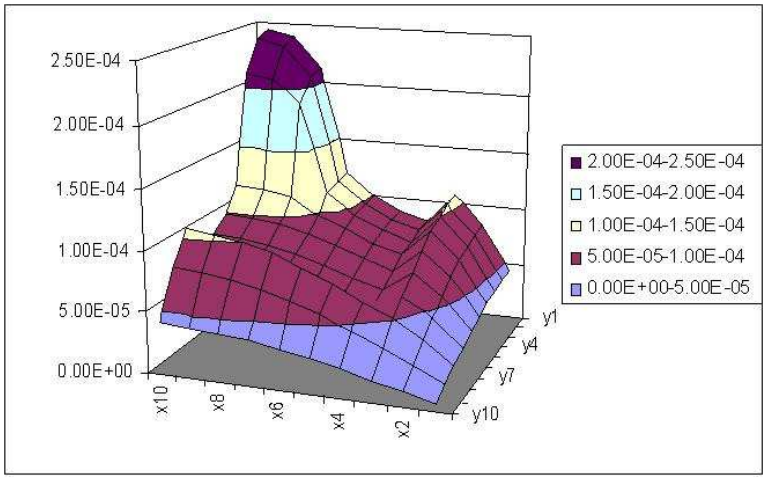

Figure 7: MOCK-3D Group 2 Steady State Scalar Flux Distribution for 2D TWIGL with 8.0 cm Cell Size

Examination of the scalar flux distributions shows that, while absolute accuracy of the Model 5 results will be poor, this model nonetheless captures the dominant physical effects in the TWIGL problem, most notably the neutron scalar flux peaks at the boundaries of the blanket regions and a large spike in the thermal neutron scalar flux in the central blanket region.

4.3 Null Transient Calculations

Having generated the initial equilibrium reactor state for the 2D TWIGL problem via MOCK-3D, a series of null transient computations was performed. In these calculations the specified material perturbation is not introduced to the time-dependent reactor; instead, the initial reactor state is projected forward in time via MOCK-3DK. These simulations are intended to assess whether MOCK-3DK correctly captures some fundamental reactor phenomena; i.e., that a sub-critical reactor will show a decrease in total core power over time, while in a critical reactor the power will remain constant. Four null transient cases were considered, as described in Table 6.

Table 6: Input Models used in MOCK-3D for 2D TWIGL Null Transient Study

Case	Angular Flux Approximation	Material State	Cell Model
Case 1	Constant	Sub-Critical	Model 5
Case 2	Constant	Critical	Model 5
Case 3	Linear	Sub-Critical	Model 5
Case 4	Linear	Critical	Model 5

Computation of these null transient cases provides a useful tool to assess the numerical stability problem that was identified and discussed in Section 3.2. Computations were attempted for time step sizes ranging between 10^{-3} seconds and 10^{-8} seconds and, as seen in Table 7, the existence of a minimum time step threshold at approximately the expected order of magnitude was verified.

Table 7: Stability of MOCK-3D Computations during 2D TWIGL Null Transient Study

Δt (sec)	Constant Flux Approximation		Linear Flux Approximation	
	Critical	Sub-Critical	Critical	Sub-Critical
10^{-3}	Stable	Stable	Stable	Stable
10^{-4}	Stable	Stable	Stable	Stable
10^{-5}	Stable	Stable	Stable	Stable
10^{-6}	Unstable	Stable	Stable	Stable
10^{-7}	Unstable	Unstable	Unstable	Unstable
10^{-8}	Unstable	Unstable	Unstable	Unstable

A computation of 200 time steps was completed for each of the stable cases listed in Table 7. From plots of the total core power versus time for each of these cases, it was determined that the MOCK-3DK null transients yield the expected physical behavior – total power decreases linearly for all of the sub-critical reactor cases and remains constant in the critical reactor cases. A difference was also observed between results that are computed using the constant angular flux approximation and those computed via the linear angular flux approximation; however, it is necessary to use a more refined spatial model – and, therefore, substantially increase the computational efficiency of the MOCK-3DK computational procedures – before a meaningful assessment can be completed in regards to these numerical effects.

4.4 Step and Ramp Transient Calculations

The step and ramp transient calculations specified in Section 4.1 were performed for three different time step sizes: $5x10^{-3}$ seconds, $5x10^{-4}$ seconds, and $5x10^{-5}$ seconds. The duration of all calculations was again limited to 200 time steps and results are presented for the problem state equivalent to null transient Case 2: the simplest angular flux approximation (constant) is utilized and the material perturbation is induced in a critical reactor. For the step transient, which yielded a linear trend in total core power, plots of total power were extrapolated to a total problem time of 1.0 seconds, as shown in Figure 8.

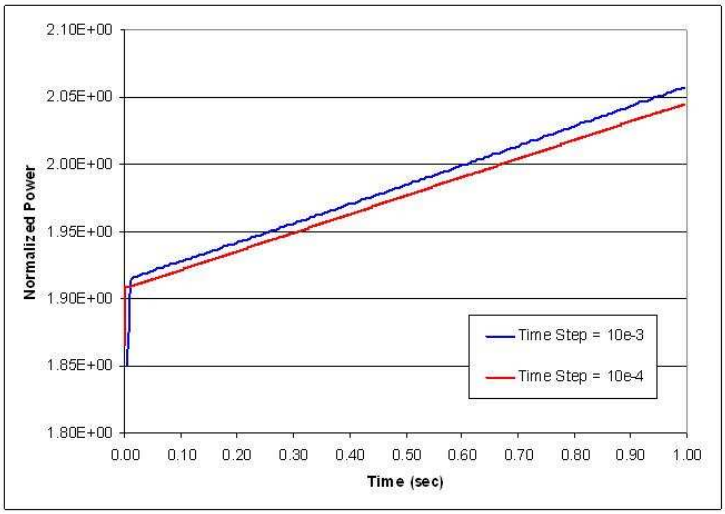

Figure 8: Extrapolated Power versus Time for 1.0 sec of 2D TWIGL Step Transient

Total core power for the ramp transients is plotted in Figure 9. These trends are not linear and the results could not be extrapolated beyond the computed 200 time steps; thus, while the trends are plotted together for convenience, each uses a different time scale and quantitative comparison of these trends is not implied.

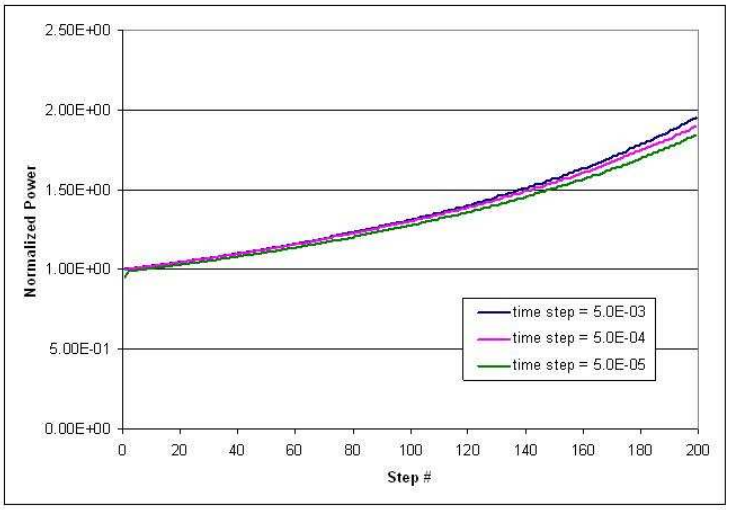

Figure 9: MOCK-3D Normalized Power for 200 Time Steps of 2D TWIGL Ramp Transient

A snapshot of the 2D scalar flux distribution was produced for each of the step and ramp transient calculations identified above. In every case the shape of this profile was similar to that shown in Figure 6 and Figure 7. A qualitative assessment the effects of the step transient on the localized scalar flux distribution is achieved by computing the percent change in scalar flux at each computational point between the beginning and endpoints of the transient calculation. Figure 10 and Figure 11 show plots of these differences for the step change transient with 10^{-4} second time steps. Similar scalar flux change distributions were found to result for all of the step and ramp transients.

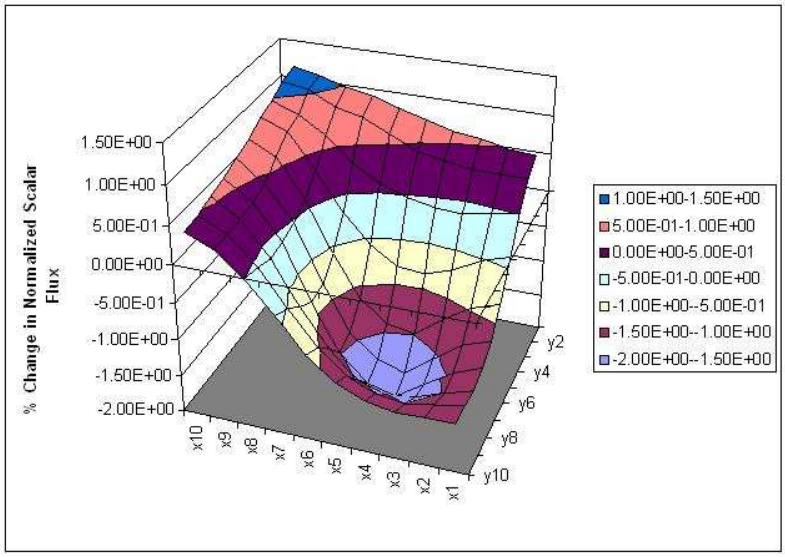

Figure 10: Percent Difference between MOCK-3D Group 1 Scalar Flux Values at t = 0 and after 200 Time Steps of 2D TWIGL Step Transient

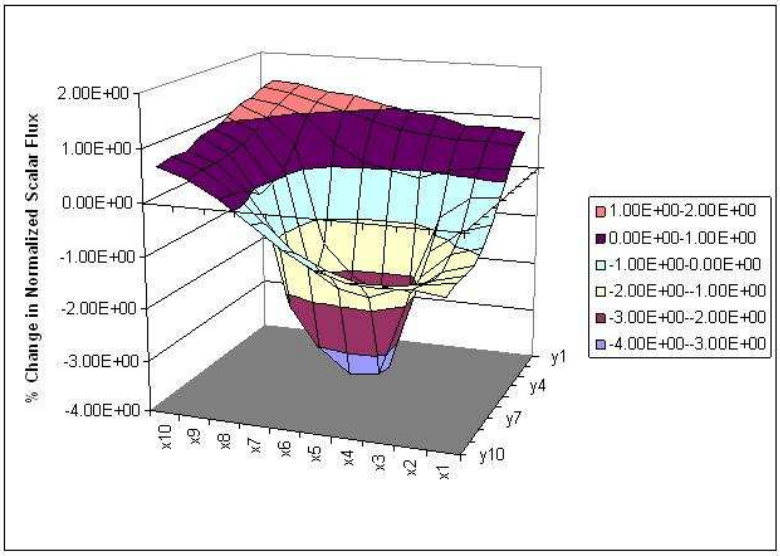

Figure 11: Percent Difference between MOCK-3D Group 2 Scalar Flux Values at t = 0 and after 200 Time Steps of 2D TWIGL Step Transient

While the coarse spatial model used in calculating the step and ramp transients resulted in poor absolute accuracy of the resulting MOCK-3DK solution, as discussed previously, the results shown above demonstrate that the fully implicit method of characteristics is again capturing the dominant physical phenomena for this problem. Total core power in all cases exhibits the behavior that would be expected for a super-critical transient – i.e., a linear increase in power where reactivity is inserted as a step change at t = 0 and a non-linear increase when a ramped reactivity insertion is introduced. Notably, Figure 10 and Figure 11 demonstrate that the localized affects of the material perturbation cause a depression in the scalar flux at the location of the perturbation, as would be expected. It can be concluded, therefore, that the method of characteristics is capable of modeling this transient and that most of the inaccuracy is a direct result of the computational expense associated with this method.

5. CONCLUSIONS

A complete theoretical derivation of a fully implicit method of characteristics formulation, its implementation into the MOCK-3D reactor kinetics code package, and subsequent application to the 2D TWIGL problem provide the first evidence of feasibility for a time-dependent method of characteristics computation; however, this method is extremely computationally expensive and practical application will require the introduction of computational acceleration and/or parallel processing. As appropriate acceleration and parallelization techniques have been previously developed for the 3D steady state method of characteristics [18,19], the problem of computational expense is not expected to be insurmountable. A more significant issue raised by this investigation regards the peculiar numerical instability that results from the application of time-differencing to the method of characteristics. While this instability can be mitigated by careful modeling of the problem geometry and selection of appropriate time step sizes, the existence of such an issue suggests that finite differencing of the temporal domain may not be the most appropriate means for solving the time-dependent characteristics equation. Future research should, therefore, investigate alternative means for discretizing the temporal domain. Alternatively, if finite differencing is found to be adequate, the problem of selecting an appropriate spatial approximation for the angular flux should be more carefully examined once more accurate results can be obtained.

REFERENCES

1. A. PAUTZ and A. BIRKHOFER, “DORT-TD: A Transient Neutron Transport Code with Fully Implicit Time Integration,” *Nucl. Sci. Eng.*, v**145**, pp.299-319 (2003).
2. S. GOLUOGLU and H. L. DODDS, “A Time-Dependent, Three-Dimensional Neutron Transport Methodology,” *Nucl. Sci. Eng.*, v**139**, pp.248-261 (2001).
3. R. G. MCCLARREN, J. P. HOLLOWAY, T. A. BRUNNER, and T. A. MELHORN, “Quasilinear Implicit Riemann Solver for the Time-Dependent P_n Equations,” *Nucl. Sci. Eng.*, v**155**, pp.290-299 (2007).
4. E. M. GELBARD, "Application of Spherical Harmonics Method to Reactor Problems," WAPD-BT-20 (Sept 1960).
5. K. S. SMITH, "Multidimensional Nodal Transport Using the Simplified P_L Method," *Proc. Joint Int. Conf. Mathematical Methods and Supercomputing for Nuclear Applications*, Saratoga Springs, New York, October 5-9, 1997, p223 (1997).
6. A. RINEISKI, J. Y. DORIATH, *Proc. Joint Int. Conf. Mathematical Methods and Supercomputing for Nuclear Applications*, Saratoga Springs, New York, October 5-9, 1997, v**2**, p1661 (1997).
7. J. B. TAYLOR, D. KNOTT, and A. B. BARATTA, “A Method of Characteristics Solution to the OECD/NEA 3D Neutron Transport Benchmark Problem,” *Joint International Topical Meeting on Mathematics &*

Computation and Supercomputing in Nuclear Applications (M&C + SNA 2007), Monterey, California, April 15-19, 2007, on CD-ROM, American Nuclear Society, LaGrange Park, IL (2007).
8. Y. H. KIM and N. Z. CHO, "A Bilinear Weighting Method for the Control Rod Cusping Problem in Nodal Methods," *J. Korean Nucl. Soc.*, v**22**, n3, pp.238-249 (1990).
9. N. Z. CHO, G. S. LEE, and C. J. PARK, "Fusion of Method of Characteristics and Nodal Method for 3D Whole-Core Transport Calculation," *Trans. Am. Nucl. Soc.*, v**86**, pp.322-324 (2002).
10. I. R. SUSLOV, O. G. KOMLEV, N. N. NOVIKOVA, E. A. ZEMSKOV, I. V. TORMYSHEV, K. G. MEL'NIKOV, and E. B. SIDOROV, "Method of Characteristics for Calculation of VVER without Homogenization," *Proc. Int. Conf. Mathematics and Computation, Supercomputing, Reactor Physics and Nuclear and Biological Applications*, Palais des Papes, Avignon, France, September 12-15, 2005 (2005).
11. G. J. WU and R. ROY, "A New Characteristics Algorithm for 3D Transport Calculations," *Ann. Nucl. Energy*, v**30**, p.1 (2003).
12. M. HURSIN, S. XIAO, and T. JEVREMOVIC, "Synergism of the Method of Characteristic, R-functions and Diffusion Solution for Accurate Representation of 3D Neutron Interactions in Research Reactors using the AGENT Code System," *Ann. Nucl. Energy*, v**33**, pp.1116-1133 (2006).
13. J. B. TAYLOR, "The Development of a Three-Dimensional Nuclear Reactor Kinetics Methodology Based on the Method of Characteristics," PhD Thesis, The Pennsylvania State University (2007).
14. T. M. SUTTON and B. N. AVILES, "Diffusion Theory Methods for Spatial Kinetics Calculations," *Prog. in Nucl. Energy*, v**30**, n2, pp.119-182 (1996).
15. W. M. STACEY, JR., *Space-Time Nuclear Reactor Kinetics*, Academic Press, New York (1969).
16. D. R. FERGUSON and K. L. DERSTINE, "Optimized Iteration Strategies and Data Management Considerations for Fast Reactor Finite Difference Diffusion Theory Codes," *Nucl. Sci. and Eng.*, v**64**, pp.593-604 (1989).
17. L. A. HAGEMAN and J. B. YASINSKY, "Comparison of Alternating-Direction Time-Differencing Methods with Other Implicit Methods for the Solution of the Neutron Group-Diffusion Equations," *Nucl. Sci. Eng.*, v**38**, p.8 (1969).
18. M. R. ZIKA, "Iterative Acceleration for Two-Dimensional Long-Characteristics Transport Problems," PhD Thesis, Texas A&M University (1997).
19. M. DAHMANI and R. ROY, "Parallel Solver Based on the Three-Dimensional Characteristics Method: Design and Performance Analysis," *Nucl. Sci. Eng.*, v**150**, pp.1-15 (2005).